Supplementary information to

Newly detected ozone depleting substances in the atmosphere

Johannes C. Laube, Mike J. Newland, Christopher Hogan, Carl A. M. Brenninkmeijer, Paul J. Fraser, Patricia Martinerie, David E. Oram, Claire E. Reeves, Thomas Röckmann, Jakob Schwander, Emmanuel Witrant and William T. Sturges

Text summary

This supplement is divided into seven sections. In Section 1, further information on reported production and imports, as obtained from the Ozone Secretariat, is discussed. In the case of CFC-112/CFC-112a these data are compared to the emissions inferred from atmospheric measurements. Section 2 shows and discusses an additional data set originating from measurements on samples collected mainly in the upper troposphere in the frame of the CARIBIC project (www.caribic-atmospheric.com). Section 3 mainly discusses quantitative data related to the Cape Grim record including growth rates and annual mixing ratios. The methodologies for the estimation of stratospheric lifetimes and Ozone Depletion Potentials (ODPs) are described in Section 4 and Section 5 provides details on the identification and quantification methods of the four compounds. Section 6 and 7 explain details of the firn as well as the emission modelling methods.

1. Discussion on production and imports

Displayed in Figure S1 is the information received from the Ozone Secretariat on production and import of CFC-112. Note, that imports are not reported as net production above values reported as production so the possibility of a double count cannot be ruled out. As stated in the main manuscript, isomeric compounds do not have to be reported separately, so when comparing the atmospheric emissions inferred here with these reports we take the sum of CFC-112 and CFC-112a. According to the Ozone Secretariat significant amounts of CFC-112/112a were still being produced from 1989 up until 2001 with imports of up to 533 tonnes per year after that period. Production and imports could however only account for the cumulative emissions inferred from observations if (a) a large part was released directly into the atmosphere or (b) production was much higher before 1988. For CFC-113a and HCFC-133a reports are much more fragmentary with only one import of CFC-113a reported in 2011 and one country reporting production of 1490 t of HCFC-133a in 2010. In accordance with the Montreal Protocol these data has been anonymised which precludes further discussions.

It should be noted, that our observations do not prove that CFC-112, CFC-112a, CFC-113a, and HCFC-133a are entirely man-made. If these substances are not conserved in firn air, or if they are produced by biologically mediated processes that have been enhanced in recent years such as by climate change, then there could be an alternate explanation for the observations reported here. Such alternate explanations cannot be entirely excluded but are very unlikely given the evidence for the industrial usage of these compounds.

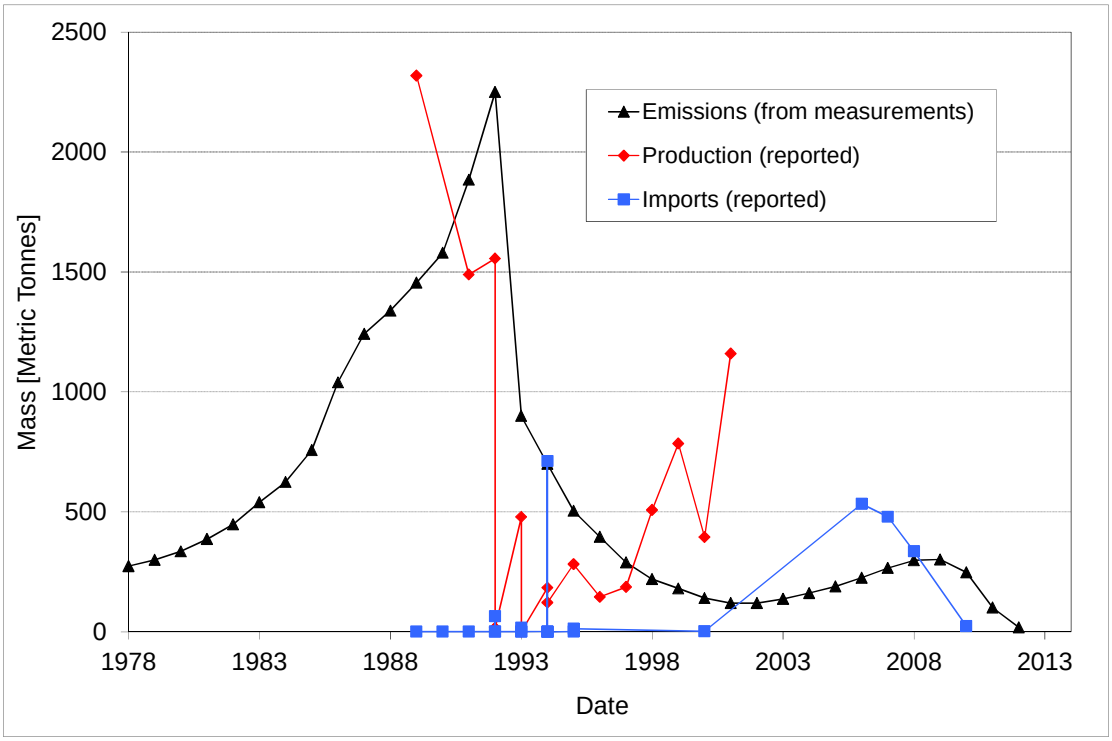

Figure S1. Emissions inferred from atmospheric measurements (black, see also Sections 3 and 7 in this supplement) as well as imports and production reported to the Ozone Secretariat for the sum CFC-112 and CFC-112a.

2. Discussion of additional measurements

The four compounds were also measured in air samples collected on board regular passenger aircraft flights in the frame of the CARIBIC project (www.caribic-atmospheric.com). The analysed samples originate from flights in 2009, 2010, and 2011 from Frankfurt (Main), Germany to Cape Town and Johannesburg, South Africa. The results are shown in Figure S2 to S5. Consistent with the Cape Grim record, we do not find indications for interhemispheric gradients or growth between 2009 and 2011 for CFC-112 and CFC-112a. For the latter we however observe mixing ratios that are consistently around 20 % higher than those retrieved from the other data sets (i.e. the Cape Grim record, the firn record, and in the vicinity of the tropopause for the stratospheric samples). This is an indication of a possible interference in these

samples which causes a bias in CFC-112a mixing ratios, but we note that all CFC-112a data sets agree within their 2 σ measurement uncertainties.

For CFC-113a and HCFC-133a we find consistency between all data sets and in addition interhemispheric gradients as well as tropospheric growth as apparent from Figures S4 and S5. For HCFC-133a we additionally find a strong increase of mixing ratios in the Northern Hemisphere in March 2011. It should have reached the Cape Grim observatory at the end of our current record in December 2012. Mixing ratios observed at Cape Grim came close to 0.4 ppt in 2012 but showed no further acceleration of the global atmospheric growth of HCFC-133a. Given these abundances we conclude that this increase was not representative of a large region.

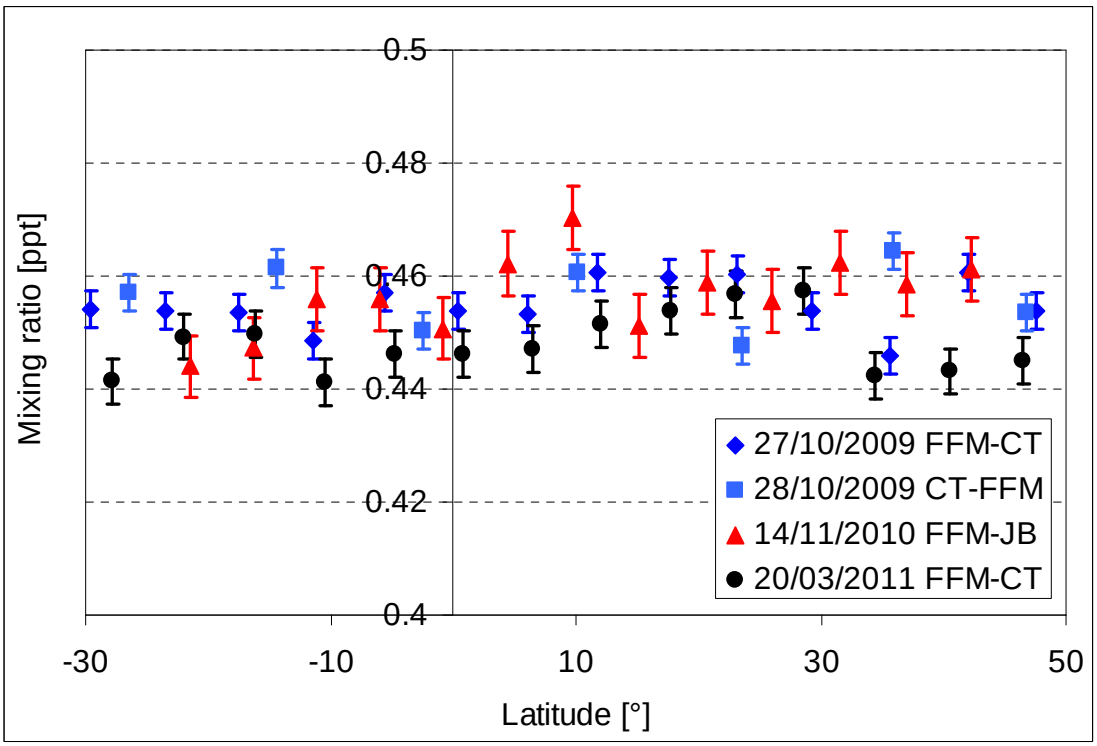

Figure S2. Mixing ratios of CFC-112 as observed in air samples collected in the troposphere (collection altitude range 8.6 - 12.2 km) during passenger aircraft flights from Frankfurt (Main), Germany (FFM) to Cape Town (CT) and Johannesburg (JB), South Africa. The error bars represent the respective 1 σ measurement uncertainties.

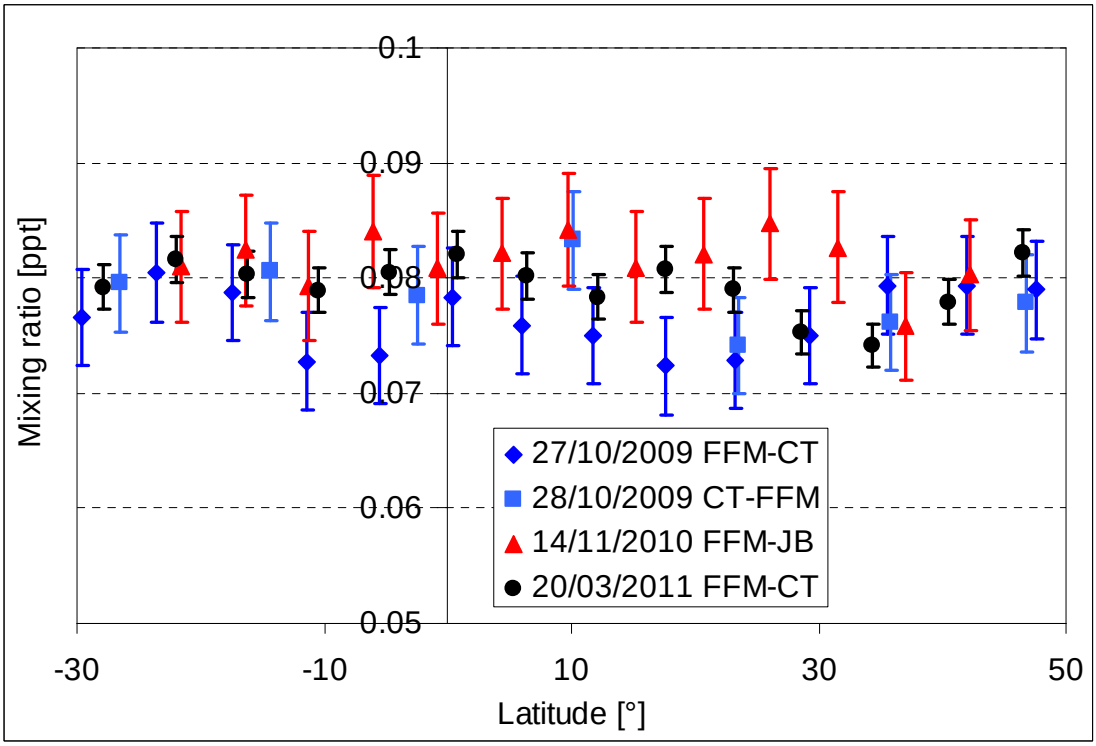

Figure S3. The same as in Figure S2 but for CFC-112a.

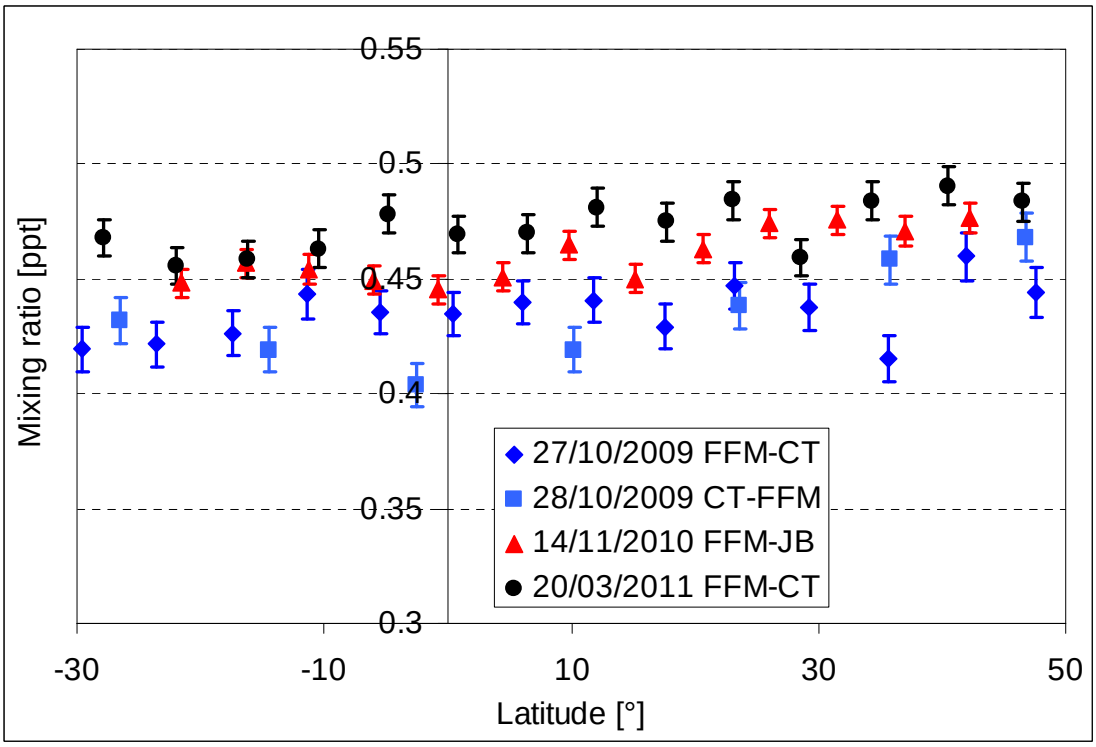

Figure S4. The same as in Figure S2 but for CFC-113a.

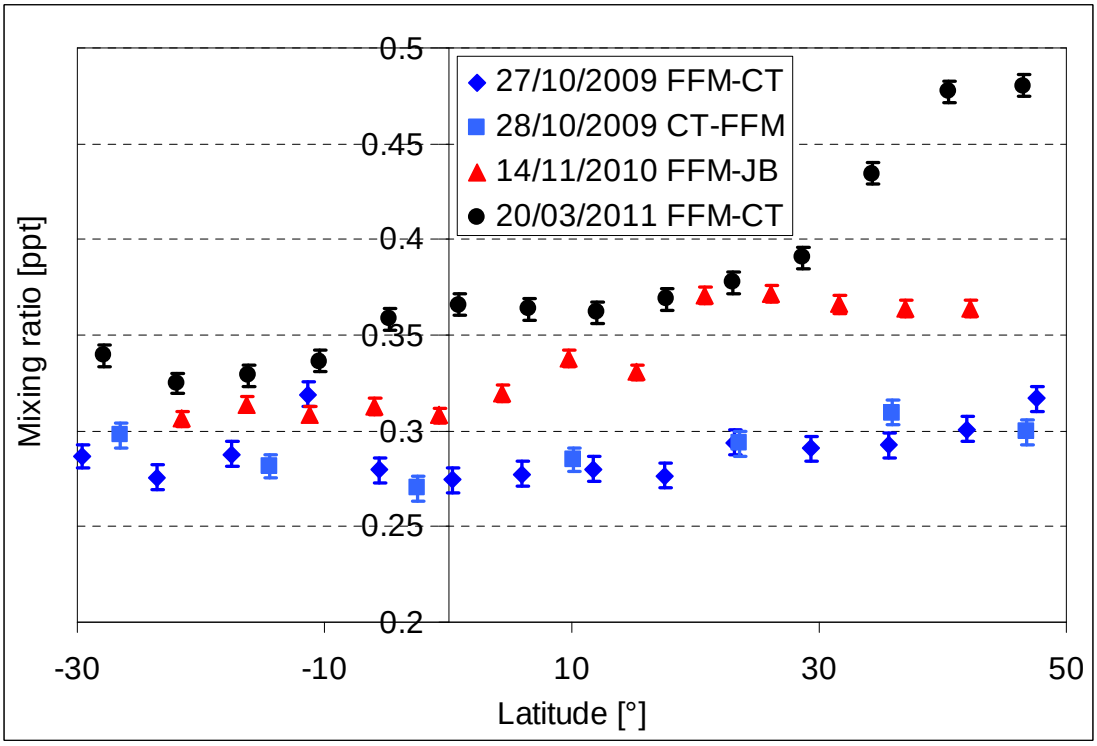

Figure S5. The same as in Figure S2 but for HCFC-133a.

3. Discussion of growth rates, annual mixing ratios, and emissions from the Cape Grim data set

Figure S6 shows the evolution of growth rates for CFC-112 and CFC-112a after 2000. These growth rates were derived directly from the mixing ratios of the Cape Grim samples by fitting linear regression lines over 5 year periods. The slope of these regression lines is the average growth rate. The Figure demonstrates a significant increase in growth rate for these two molecules after 2005 followed by a decrease from around 2010 which support the hypothesis of increasing and later decreasing emissions suggested by the more indirect method of emission modelling.

Table S1 details the annual mixing ratios inferred from fits to the Cape Grim data as well as the respective global emissions of CFC-112, CFC-112a, CFC-113a, and HCFC-133a. Emission uncertainties were inferred using the 1 σ measurement uncertainties as well as the uncertainty ranges of the lifetime estimates (see also

Section 7 of this supplement). In the case of HCFC-133a where tropospheric reaction with OH is the dominant sink we also considered the uncertainty in the OH concentration and in the respective reaction rate coefficient.

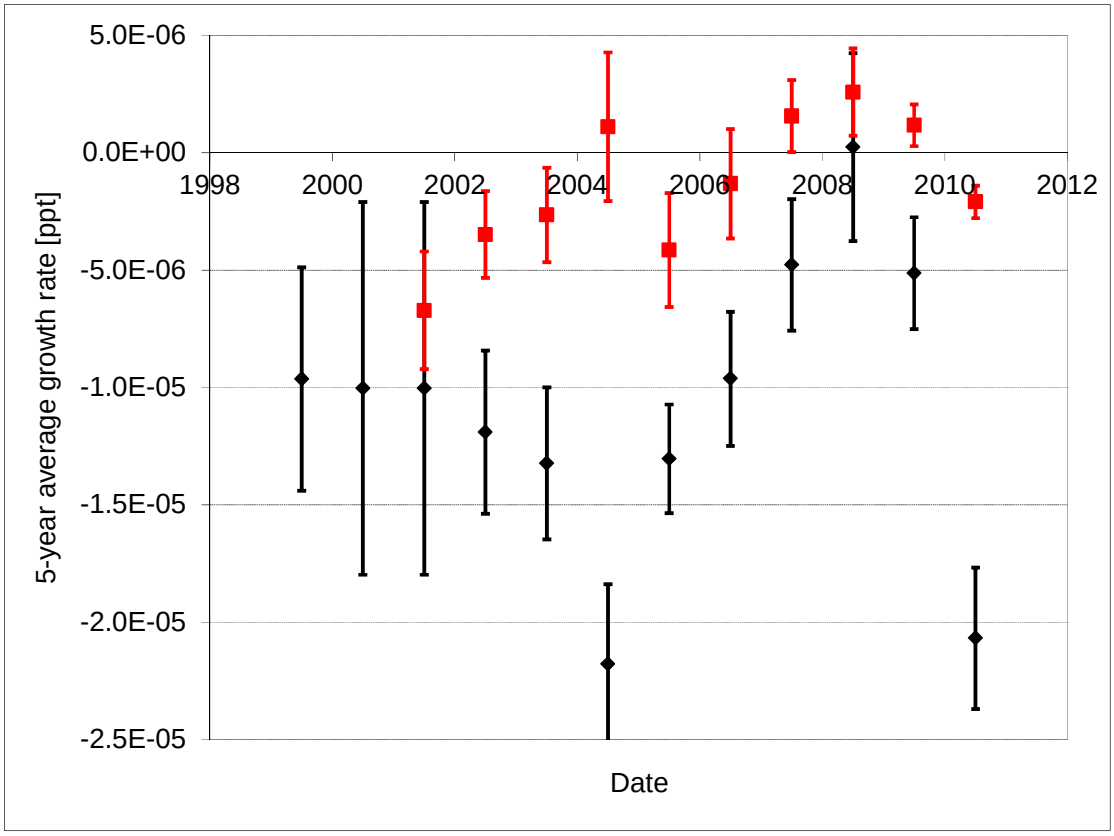

Figure S6. Average growth rates of CFC-112 (black) and CFC-112a (red) as directly inferred from the Cape Grim measurements. Growth rates were derived as the slopes of the sample mixing ratios by fitting linear regression over 5 year periods. The error bars represent the 1 σ slope uncertainties.

Table S1. Annual average mixing ratios from fits to the Cape Grim air archive measurements. Average 1 σ measurement uncertainties of these fits are 0.011 ppt for CFC-112, 0.004 ppt for CFC-112a, 0.010 ppt for CFC-113a, and 0.003 ppt for HCFC-133a. Also shown are the respective estimated global emissions and their uncertainties.

Emissions of CFC-112a prior to 1999 were inferred from firn air data and sum up to 3.26 Gg.

Year	Cape Grim mixing ratio from fit [ppt]	Global emissions [Gg]	Emission uncertainty range [Gg]
CFC-112			
1978	0.092	0.27	0.24-0.31
1979	0.098	0.30	0.26-0.34
1980	0.105	0.34	0.29-0.38
1981	0.112	0.39	0.34-0.44
1982	0.121	0.45	0.39-0.51
1983	0.132	0.54	0.47-0.62
1984	0.145	0.63	0.55-0.71
1985	0.160	0.76	0.70-0.82
1986	0.179	1.04	0.97-1.12
1987	0.205	1.24	1.18-1.31
1988	0.236	1.34	1.27-1.40
1989	0.270	1.46	1.38-1.52
1990	0.307	1.58	1.48-1.64
1991	0.347	1.88	1.77-1.95
1992	0.395	2.25	2.18-2.29
1993	0.444	0.90	0.82-1.05
1994	0.471	0.70	0.60-0.80
1995	0.485	0.50	0.41-0.63
1996	0.491	0.40	0.30-0.51
1997	0.494	0.29	0.18-0.43

1998	0.493	0.22	0.10-0.37
1999	0.491	0.18	0.05-0.33
2000	0.487	0.14	0.03-0.29
2001	0.481	0.12	0.01-0.27
2002	0.476	0.12	0.01-0.25
2003	0.470	0.12	0.01-0.24
2004	0.464	0.13	0.01-0.24
2005	0.459	0.15	0.02-0.26
2006	0.454	0.18	0.04-0.29
2007	0.450	0.22	0.10-0.32
2008	0.447	0.25	0.10-0.34
2009	0.446	0.26	0.10-0.35
2010	0.444	0.21	0.03-0.32
2011	0.441	0.08	0.00-0.27
2012	0.436	0.01	0.00-0.19
CFC-112a			
1999	0.075	0.00	0.00-0.04
2000	0.073	0.00	0.00-0.04
2001	0.071	0.00	0.00-0.04
2002	0.070	0.00	0.00-0.04
2003	0.068	0.02	0.01-0.06
2004	0.067	0.03	0.01-0.07
2005	0.067	0.04	0.02-0.08
2006	0.066	0.05	0.02-0.08
2007	0.066	0.05	0.02-0.09

2008	0.066	0.05	0.02-0.08
2009	0.066	0.04	0.01-0.08
2010	0.066	0.03	0.00-0.07
2011	0.065	0.02	0.00-0.05
2012	0.065	0.01	0.00-0.03
CFC-113a			
1978	0.040	0.34	0.28-0.37
1979	0.050	0.35	0.29-0.39
1980	0.060	0.36	0.30-0.42
1981	0.070	0.36	0.31-0.43
1982	0.080	0.36	0.31-0.43
1983	0.090	0.36	0.31-0.42
1984	0.100	0.37	0.30-0.42
1985	0.110	0.37	0.30-0.43
1986	0.120	0.38	0.31-0.45
1987	0.129	0.40	0.33-0.48
1988	0.139	0.42	0.36-0.49
1989	0.150	0.43	0.37-0.51
1990	0.161	0.45	0.39-0.55
1991	0.172	0.46	0.38-0.57
1992	0.183	0.47	0.38-0.58
1993	0.195	0.48	0.39-0.60
1994	0.206	0.49	0.39-0.61
1995	0.218	0.51	0.42-0.65
1996	0.229	0.52	0.43-0.67

1997	0.241	0.53	0.44-0.69
1998	0.254	0.54	0.44-0.71
1999	0.266	0.55	0.44-0.73
2000	0.278	0.57	0.44-0.75
2001	0.291	0.58	0.43-0.77
2002	0.303	0.59	0.43-0.78
2003	0.316	0.60	0.44-0.79
2004	0.329	0.61	0.45-0.79
2005	0.342	0.63	0.46-0.81
2006	0.356	0.65	0.48-0.83
2007	0.369	0.68	0.51-0.86
2008	0.384	0.73	0.55-0.91
2009	0.399	0.79	0.60-1.03
2010	0.416	0.87	0.65-1.11
2011	0.439	1.70	1.50-1.85
2012	0.479	2.00	1.80-2.70
HCFC-133a			
1978	0.018	0.13	0.10-0.18
1979	0.019	0.14	0.11-0.20
1980	0.020	0.15	0.12-0.21
1981	0.022	0.16	0.12-0.22
1982	0.024	0.17	0.13-0.24
1983	0.025	0.18	0.14-0.25
1984	0.027	0.19	0.15-0.27
1985	0.029	0.20	0.15-0.28

1986	0.031	0.23	0.18-0.32
1987	0.033	0.26	0.20-0.36
1988	0.036	0.29	0.22-0.41
1989	0.040	0.32	0.24-0.45
1990	0.044	0.36	0.28-0.50
1991	0.049	0.40	0.31-0.55
1992	0.054	0.46	0.35-0.63
1993	0.061	0.54	0.41-0.73
1994	0.069	0.61	0.47-0.83
1995	0.077	0.61	0.47-0.83
1996	0.085	0.61	0.46-0.83
1997	0.091	0.61	0.45-0.83
1998	0.096	0.65	0.48-0.88
1999	0.102	0.73	0.54-1.01
2000	0.108	0.65	0.48-0.90
2001	0.111	0.65	0.48-0.90
2002	0.114	0.65	0.48-0.90
2003	0.118	1.00	0.75-1.35
2004	0.134	1.70	1.35-2.22
2005	0.168	2.10	1.78-2.35
2006	0.212	2.40	1.96-3.25
2007	0.255	2.00	1.60-2.60
2008	0.276	1.00	0.58-1.65
2009	0.268	1.10	0.65-1.70
2010	0.270	3.10	2.70-3.70

2011	0.316	3.10	2.45-4.10
2012	0.368	3.10	2.50-3.80

4. Methods to calculate stratospheric lifetimes and ODPs

Stratospheric lifetimes τ were calculated using Eq. S1 as taken from [10] (cf. Eq. 6) which is based on [11].

$$\tau_i = \tau_{CFC-11} \cdot \frac{\overline{\sigma}_i}{\overline{\sigma}_{CFC-11}} \cdot \frac{-20.6 + \gamma_{0,CFC-11} \cdot \sigma_{0,CFC-11}}{-20.6 \cdot \frac{d\chi_i}{d\chi_{CFC-11}} + \gamma_{0,i} \cdot \sigma_{0,i}} \cdot \frac{1 - 2 \cdot \gamma_{0,i} \cdot \Lambda}{1 - 2 \cdot \gamma_{0,CFC-11} \cdot \Lambda} \qquad \text{(S1)}$$

$\overline{\sigma}$ - average atmospheric mixing ratio in steady state

$\frac{d\chi_i}{d\chi_{CFC-11}}$ - slope of the mixing ratio correlation at the extratropical tropopause

σ - steady-state mixing ratio (index 0 = at the tropopause)

γ_0 - effective linear tropospheric growth rate in year^{-1} (cf. [11], Eq. A13)

Λ - ratio of the squared width of the age spectrum Δ^2 to mean age Γ; here: 1.25

Compact correlations occur in the stratosphere between two trace gases with sufficiently long lifetimes and the slope of these correlations at the tropopause is related to their stratospheric lifetimes. Figures S7 to S10 show the correlations of the four newly detected compounds with CFC-11 in air samples collected onboard the high altitude research aircraft M55-Geophysica in the extra-tropical stratosphere during deployments in late 2009 and early 2010. Also shown are the average slopes at different points of these correlations which were used to estimate the slope at the tropopause. Table S3 displays the additional required parameters as well as the

lifetimes and their 1 σ uncertainty ranges. Further methodological details can be found in [10].

Ozone Depletion Potentials (ODPs) were calculated using Eq. (S3) which has been adapted from [2].

$$ODP_i = \left(\alpha \cdot n_{Br,i} + n_{Cl,i}\right) \cdot \frac{FRF_i}{FRF_{CFC-11}} \cdot \frac{\tau_i}{\tau_{CFC-11}} \cdot \frac{M_{CFC-11}}{M_i} \cdot \frac{1}{3} \quad \text{(S3)}$$

α - relative ozone destruction effectiveness of bromine as compared to chlorine; here: 60 as recommended in WMO (2011) for mid latitudes

n - number of bromine/chlorine atoms

FRF – mid-latitudinal Fractional Release Factor at a mean age of 3 years

τ - overall atmospheric lifetime

M - molecular mass

A Fractional Release Factor (FRF, i.e. a quantity describing the fraction of halogen released from a trace gas at a certain time and location in the stratosphere) is needed to calculate these ODPs. Again applying the methods of [10] we infer mean stratospheric transit times (i.e. mean ages of air) and subsequently correct our measurements for changes in tropospheric trends by using the Cape Grim record (shifted by 6 months to represent the mixing ratios that entered the tropical stratosphere). Semi-empirical ODPs are calculated from the FRFs observed in the mid-latitudinal stratosphere at mean ages of 3 years[2]. We find FRFs of 0.30 (uncertainty range 0.29-0.31) for CFC-112, 0.35 (0.32-0.39) for CFC-112a, 0.29 ().27-0.31) for CFC-113a, and 0.03 (0.00-0.05) for HCFC-133a. When using these

values and the inferred atmospheric lifetimes (the one reported in [2] in the case of HCFC-133a) we calculate the ODPs given in the main manuscript.

Table S3. Additional details on stratospheric lifetime calculation.

Compound	$\bar{\sigma}$ [ppt]	γ_0 [% yr^{-1}]	$\frac{d\chi_i}{d\chi_{CFC-11}}$	τ and uncertainty range [years]	
CFC-11	227.9 ± 3.8	-0.88	1	(45)	
CFC-112	0.423 ± 0.017	-0.41	0.0017 ± 0.0006	51	(37-82)
CFC-112a	0.062 ± 0.002	-0.24	0.0003 ± 0.0002	44	(28-98)
CFC-113a	0.384 ± 0.012	3.25	0.0022 ± 0.001	51	(27-264)
HCFC-133a	0.246 ± 0.011	-1.67	0.0013 ± 0.0005	35	(21-92)

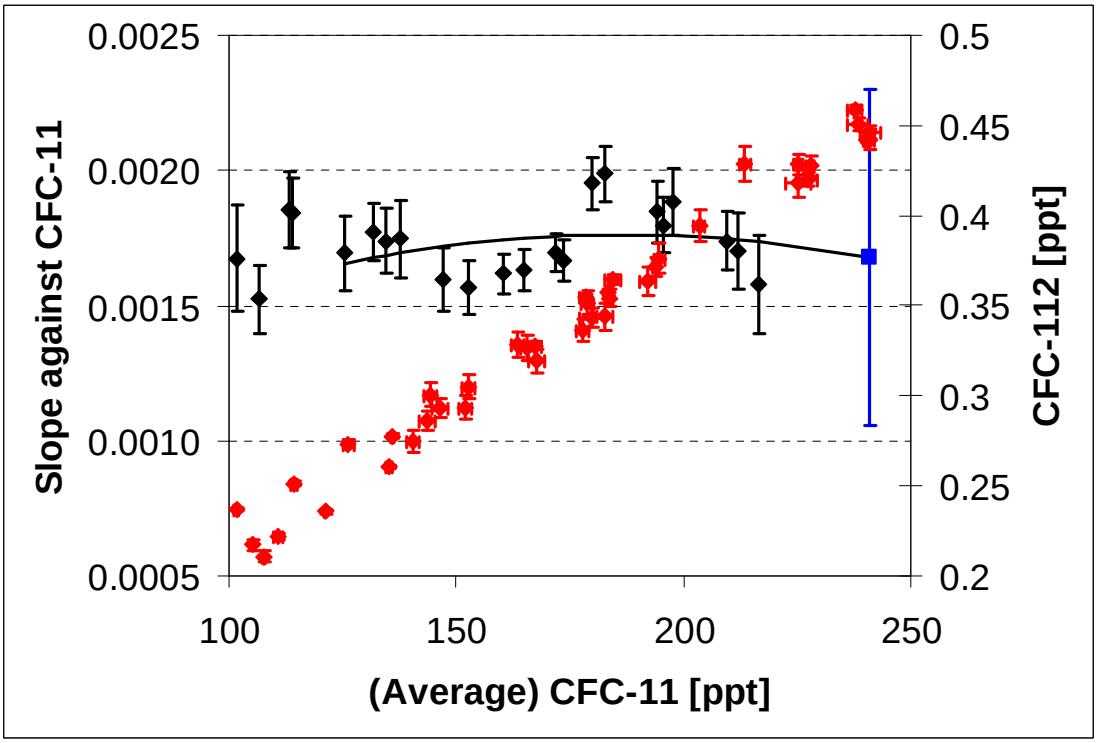

Figure S7. Correlation slopes of the mixing ratios of CFC-112 against the average mixing ratio of CFC-11. The black diamonds each represents the bivariate error-

weighted slope of the correlation inferred over a range of ± 35 ppt CFC-11. The error bars represent the 1 σ slope uncertainties. The black lines are the error-weighted quadratic polynomial fitted between 120 and 220 ppt and its respective uncertainty envelopes as inferred via the "bootstrap" method from [11]. Extrapolation of these polynomials to the tropopause at 241.0 ppt of CFC-11 results in the slopes and uncertainties (blue) given in Table S3. Displayed in red is the correlation of mixing ratios that was utilised to infer the slopes.

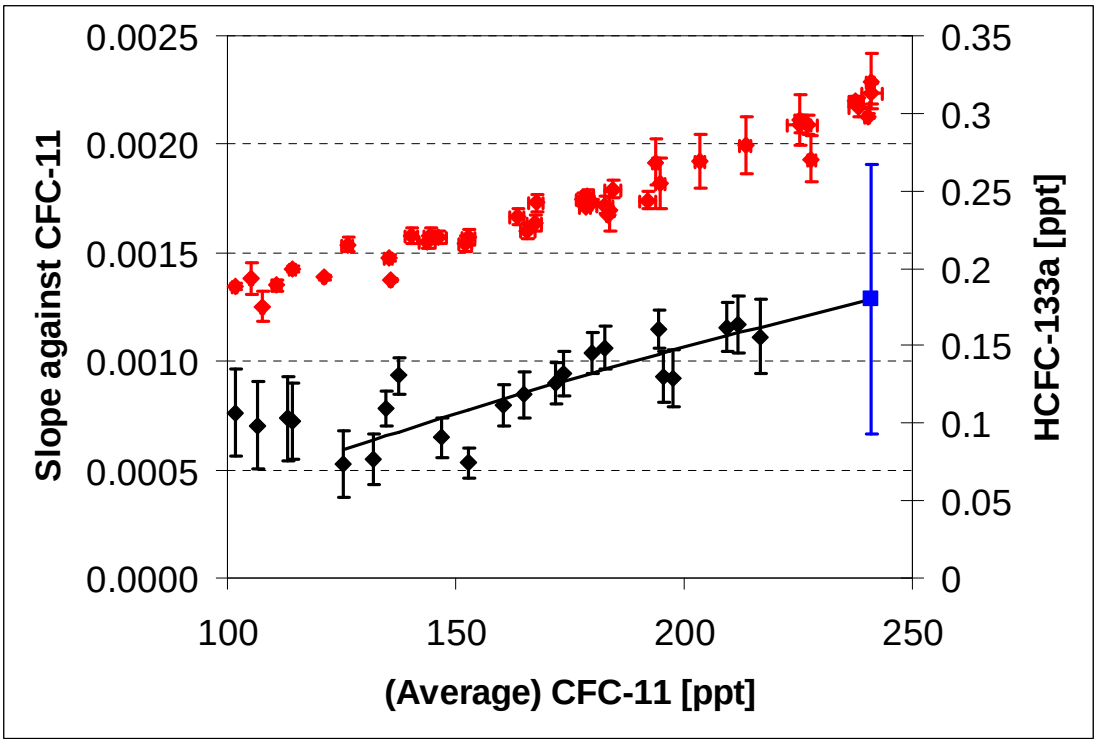

Figure S8. The same as in Figure S7 but for HCFC-133a.

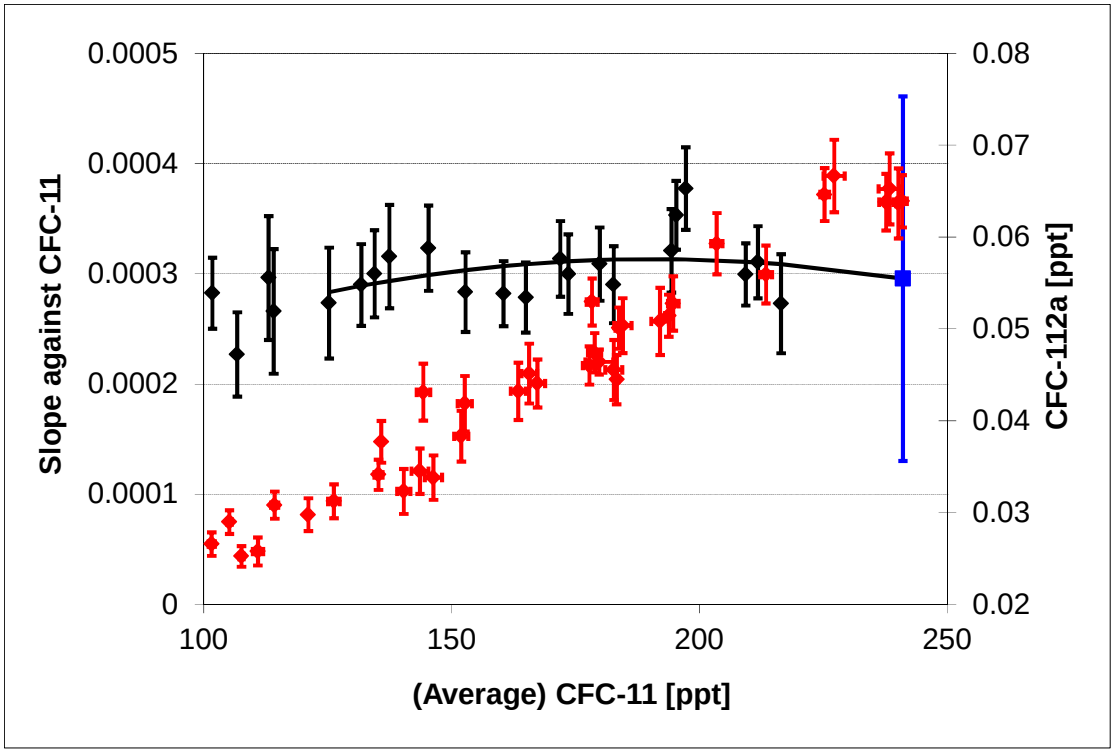

Figure S9. The same as in Figure S7 but for CFC-112a.

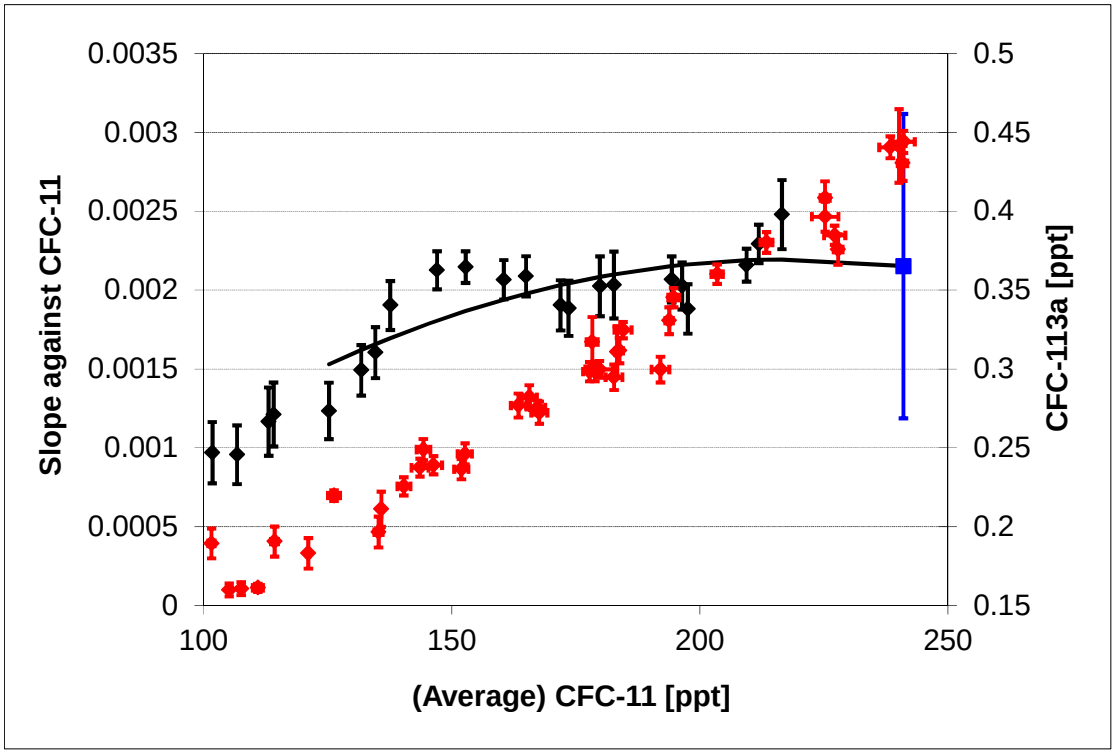

Figure S10. The same as in Figure S7 but for CFC-113a.

5. Methods to identify and quantify the newly detected compounds

Table S4 displays the quantifier and qualifier ions of the newly detected compounds. No chromatographic interferences were found for the quantifier ions at the given retention time windows. However, CFC-112a and CFC-112 elute as a double peak on the CFC-112a quantifier ion (m/z 116.91) which limits the precision of the latter. CFC-113a has a similar limitation as it forms a double peak with CFC-113 on m/z 116.91. Typical detection limits were between 0.1 and 1 part per quadrillion (ppq).

To establish calibration scales for these compounds we used the static dilution system described and evaluated in [S1] and [9]. The compounds (purity > 99 %) were obtained from DuPont (mixture of 90.8 % CFC-112 and 9.2 % CFC-112a), SIA Molport (CFC-113a), and Fluorochem Ltd. UK (HCFC-133a) and subsequently diluted in Oxygen-free Nitrogen (OFN, BOC Gases, UK) into aluminium drums (~100 litre volume) which were analysed against the working standard (i.e. compressed clean NH air) on the instrument. Internal reference compounds (i.e. CF_2Cl_2 and $CFCl_3$) were added to evaluate the quality of the dilution. These reference compounds deviated by less than 3.8 % from the well established scales of the NOAA-ESRL laboratories (NOAA-2008 for CF_2Cl_2 and NOAA-1993 for $CFCl_3$). We assign a calibration scale uncertainty of less than 7 % (similar to [9]) at the mixing ratios levels in the dilutions prepared here. The mixing ratios of the newly detected compound in the dilutions and those calculated for the working standard used to assign mixing ratios to samples (i.e. remote tropospheric air sampled in 2006) can also be found in Table S4.

The linearity of the response behaviour of the analytical system was confirmed using a static dilution series prepared by diluting an unpolluted air sample collected in 2009 at Niwot Ridge near Boulder, USA (containing 0.510 ppt of CFC-112, 0.071 ppt of CFC-112a, 0.411 ppt of CFC-113a, and 0.322 ppt of HCFC-133a) with Research

Grade Nitrogen (obtained from BOC Gases, UK) in SilcoTM-treated stainless steel canisters. Six dilutions were prepared with dilution factors of 1.00, 0.67, 0.30, 0.15, 0.07 and 0.00. Linearity was found for all four compounds within the uncertainties of the dilution factors (less than 5 % in all cases) and measurement uncertainties (see Table S4).

Table S4. Additional details on measurements and calibrations of the newly detected compounds.

Compound	CFC-112	CFC-112a	CFC-113a	HCFC-133a
Quantifier ion (m/z)	$CF^{35}Cl_2^+$ (100.94)	$C^{35}Cl_3^+$ (116.91)	$C^{35}Cl_3^+$ (116.91)	$C_2H_2F_3{}^{35}Cl^+$ (117.98)
Qualifier ion (m/z)	$C^{35}Cl_3^+$ (116.91)	$C^{35}Cl_2{}^{37}Cl^+$ (118.90)	$C^{35}Cl_2{}^{37}Cl^+$ (118.90)	$C_2H_2F_3{}^{37}Cl^+$ (119.98)
Deviation of internal std from NOAA scales [%]	-3.3 to -3.8	-3.3 to -3.8	-3.0 to -3.8	1.0 to 2.7
Mixing ratio range prepared [ppt]	9.3-13.7	0.9-1.4	23.2-34.1	19.6-30.2
Mixing ratio assigned to standard [ppt]	0.465	0.065	0.375	0.294
Typical precision of standard [%]	0.9	2.1	1.3	0.9
Standard deviation of calibrations [%]	5.8	3.5	2.3	4.1

6. Firn modelling methodology

Polar firns preserve air of increasing age with increasing depth. However trace gas concentration profiles are smoothed mainly by molecular diffusion[S2]. A state of the art model of trace gas transport in firn has been used in this study[16]; compared with other similar models in [8]). Such models need as input diffusion coefficient ratios in air of the target species with respect to CO_2. The values used calculated from critical temperature and volume data are 203.83 for CFC-112 and CFC-112a, 187.38 for CFC-113a and 118.49 for HCFC-133a, as detailed in the supplement of [8]. Forward firn models such as those inter-compared in [8] allow calculating concentrations in firn from a known atmospheric history. Reconstructing atmospheric concentration histories from depth – concentration profiles in firn requires to use inverse modelling techniques. This inverse problem has multiple solutions[S3]. A robustness oriented method for choosing the optimal solution, adapted to the scarcity of firn data (16 to 19 depth levels in this study), has been recently developed[21]. The scarcity of measurements is handled based on the mathematical development for robust solving of inverse problems from [S4]. The reconstructed scenarios, together with their match of the firn data are shown on Figures S11 and S12.

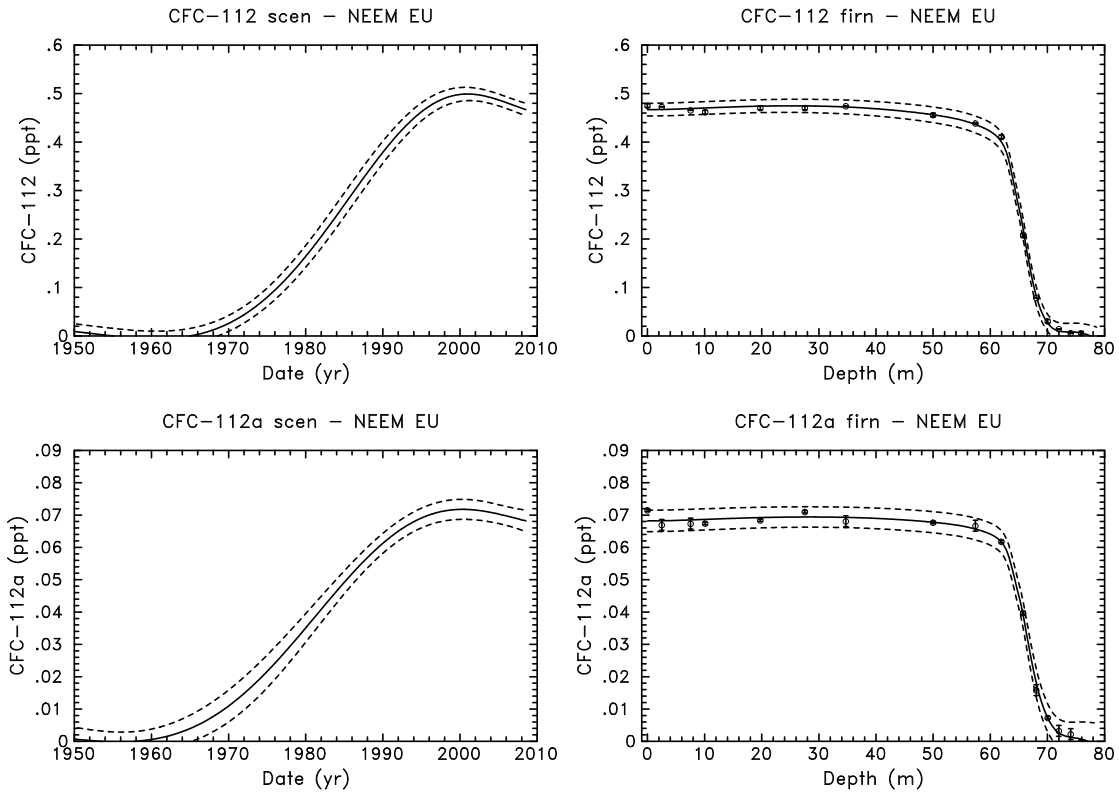

Figure S11. Reconstructed atmospheric scenarios of CFC-112 and CFC-112a (left panels) together with their match of the mixing ratios observed in firn air collected at different depth levels (right panels). The uncertainty envelopes (dashed lines) mostly reflect the differences between measured and modelled mixing ratios in firn air with an additional error propagation term[S3] inducing larger uncertainties in the deep firn air. These larger uncertainties affect the scenarios before 1950. The reconstructed scenarios are zero within error bars in their early part, reflecting the very low concentrations in firn air below 70 metres depth.

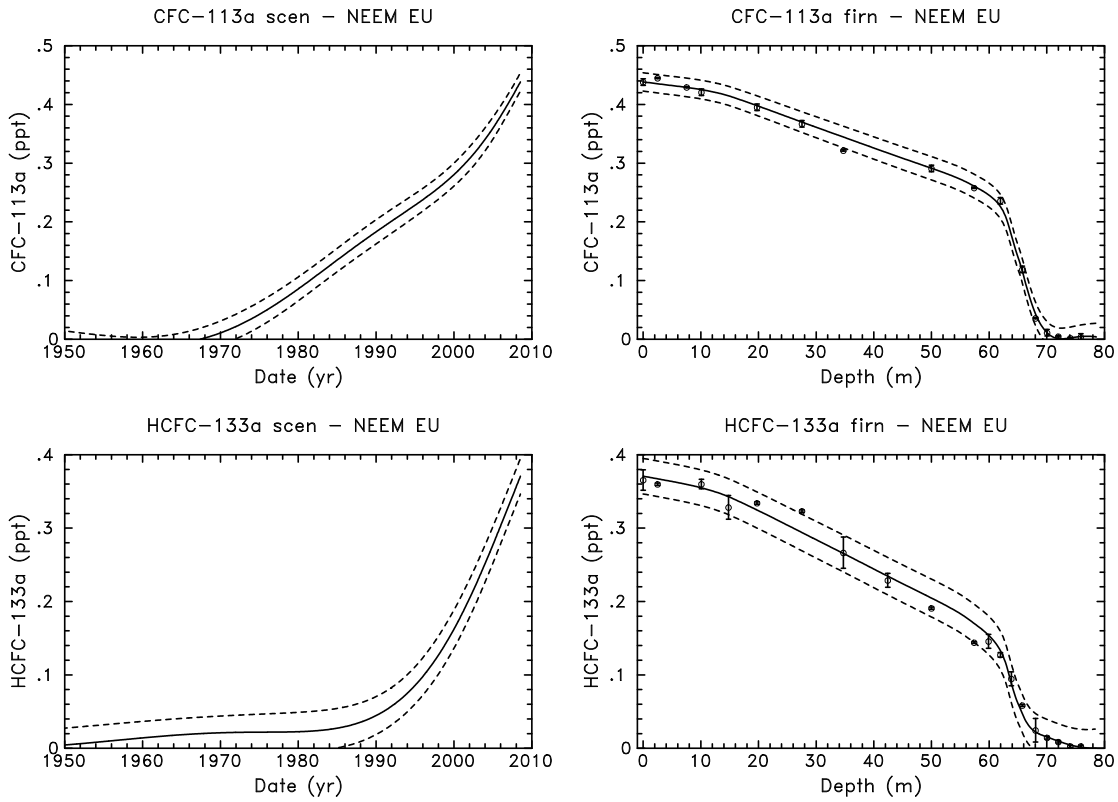

Figure S12. The same as in Figure S11 but for CFC-113a and HCFC-133a.

7. Emission modelling methodology

The emissions required to produce the temporal trend were derived using a 2-D atmospheric chemistry-transport model. The model contains 24 equal area latitudinal bands and 12 vertical levels, each of 2 km. The emissions were assigned predominantly to the northern mid-latitudes with only 4% released in the southern hemisphere. This distribution is based on [S5] and has been used previously for CFC-11 in [S6]. The model has previously been shown to reproduce southern hemispheric observations to within about 5% for gases emitted mostly in the northern hemisphere and for which there have been well reported emission inventories such as CFC-11 and CFC-12[S6].

The major sink of the CFCs is by photolysis but there are no reported absorption spectra for the three new CFCs reported here. The method described in [10] was used to

calculate stratospheric (and hence total) lifetimes of the CFCs. The diffusive loss from the top of the model was then adjusted so that the lifetime of the species within the model domain matched the lifetimes calculated by [10].

For HCFC-133a a total atmospheric lifetime of 4.3 years is reported in [2]. This is based on a combination of the lifetime with respect to OH of 4.5 years, based on the temperature dependent rate constant reported by [S7]

, $k = 1.43 \times 10^{-12}.\exp(-1400/T)$, and a stratospheric lifetime of 72 years, estimated "from an empirical correlation between the tropospheric and stratospheric lifetimes that were reported by Naik et al. (2000) for HFCs for which OH and $O(^1D)$ reaction rate constants were available". The OH reaction rate constant from [S7] was used in the model and the diffusive loss from the top of the model was then adjusted to represent the stratospheric loss and give the molecule a lifetime of 4.3 years within the model domain.

The OH field in the model was adjusted to give a partial lifetime for CH_3CCl_3, with respect to reaction with OH in agreement with [2] (6.1 years) when using a reaction rate coefficient of $1.2 \times 10^{-12}.\exp(-1440/T)$ cm^3 $molecule^{-1}$ s^{-1} [S8].

The temporal trend in the global emissions was adjusted so that the modelled mixing ratios for the latitude of Cape Grim matched the measurements of the CFCs and the HCFC. The uncertainties for the CFC emissions shown in Table S1 were calculated by running the model to fit upper and lower bounds of the measurements (defined by the mean 1-sigma measurement uncertainty) using the range of the lifetime uncertainties. The upper estimates of the emissions were therefore based on fitting the upper bound of the measurements and using the minimum value of the lifetime range, while the lower estimate of the emissions used the maximum value of the lifetime to fit to the lower bound of the measurements.

The uncertainties for the emissions of HCFC-133a were calculated by running the model to fit upper and lower bounds of the measurements (defined by the mean 1-sigma measurement uncertainty) using the range of uncertainty in the OH reaction rate coefficient as reported by [S7], which equates to about 30 %. The upper estimate of the emissions was therefore based on fitting the upper bound of the measurements and using the maximum value of the OH rate coefficient (giving a minimum lifetime), while the lower estimate of the emissions used the minimum value of the OH rate coefficient (giving a maximum lifetime) to fit to the lower bound of the measurements.

References not provided in the main manuscript:

[S1]Laube, J. C., et al. Accelerating growth of HFC-227ea (1,1,1,2,3,3,3-heptafluoropropane) in the atmosphere *Atmos. Chem. Phys.* **10**, 5903–5910 (2010)

[S2]Schwander, J. et al. The age of the air in the firn and the ice at Summit, Greenland *J. Geophys. Res.-Atmos.* **98**, 2831–2838 (1993)

[S3]Rommelaere, V., Arnaud, L., and Barnola, J. M. Reconstructing recent atmospheric trace gas concentrations from polar firn and bubbly ice data by inverse methods *J. Geophys. Res.-Atmos.* **102**, 30069–30083 (1997)

[S4]Lukas, M. A. Strong robust generalized cross-validation for choosing the regularization parameter, *Inverse Problems*, **24**, 034 006 (2008)

[S5]McCulloch, A., Midgley, P. M., and Fisher, D. A. Distribution of emissions of chlorofluorocarbons (CFCs) 11, 12, 113, 114 and 115 among reporting and non-reporting countries in 1986 *Atmos. Environ.* **28**(16), 2567–2582 (1994)

[S6]Reeves, C. E. et al. Trends of halon gases in polar firn air: implications for their emission distributions *Atmos. Chem. Phys.* **5**, 2055–2064 (2005)

[S7]Sander, S. P., J. et al. Chemical Kinetics and Photochemical Data for Use in Atmospheric Studies, Evaluation No. 17, JPL Publication 10-6, Jet Propulsion Laboratory, Pasadena (2011)

[S8]Atkinson, R. et al. Evaluated kinetic and photochemical data for atmospheric chemistry: Volume IV – gas phase reactions of organic halogen species, *Atmos. Chem. Phys*. **8**, 4141–4496 (2008)